

Supplementary Information:

Epigenetic Reprogramming of Cortical Neurons through Alteration of Dopaminergic Circuits

Karen Brami-Cherrier^{1,2}*, Andrea Anzalone^{1,2}*, Maria Ramos^{1,2*}, Ignasi Forne⁴, Fabio Macciardi^{2,3}, Axel Imhof^{2,4} and Emiliana Borrelli^{1,2}

1) Supplementary Methods

2) Supplementary Figures (1-7)

3) Supplementary Tables (1-6)

Supplementary Methods

Generation of DA-D2RKO mice

The generation and characterization of mice lacking D2R in dopaminergic neurons has been previously described¹. Briefly, D2R-floxed alleles were generated by introduction of LoxP sites on each side of a 900 bp NcoI genomic fragment of the D2R gene containing exon 2; a neomycin cassette (pGKneo), flanked by LoxP sites, was inserted at the 3' end of the NcoI genomic fragment to allow selection of the recombinant ES cells. Homozygous D2R^{flox/flox} mice were obtained (hereafter referred as WT). D2R^{flox/flox} mice were then mated with engrailed1-CRE (En1Cre) mice to generate D2R^{flox/flox/En1Cre/+} animals (hereafter referred as DA-D2RKO mice). Mutant and control mice for each line used in this study are in the same genetic background (87.5% C57BL6-12.5% 129 SV). During the establishment of the mutants, we selected by Southern analyses only mice containing the excision of the neomycine cassette. Genotyping is performed by Southern blot analyses and PCR on genomic DNA extracted from tail biopsies. Since the engrailed gene is expressed during embryonal development², D2R ablation in dopaminergic neurons of DA-D2RKO mice is achieved since early stages of development.

RNA preparation and processing for micro-arrays experiments

Total RNA was extracted using mini RNeasy kit (Qiagen), controlled using the Agilent 2100 Bioanalyzer. Probe synthesis and chip hybridization were performed by the University of California Irvine DNA Microarray Core Facility. Data were normalized, and for each probe set, the measurements of 4 (PFC) and 3 (vStr) microarrays/genotype were averaged.

Mogene (Affymetrix "MoGene 1.0 ST") chipset contains around 241000 probe sets derived from approximately 35000 mouse genes. Robust Multiarray Average normalization

(RMA) and Gene expression analyses were performed using Partek Genomics Suite software (<http://www.partek.com/>, St. Louis, MO). Significant differences between the two groups were determined by ANOVA analyses on Partek. Statistically significant genes (ANOVA) were then subjected to a post-hoc t-test and fold-change analysis (FC) in order to identify pair-wise differences between the KO and WT mice. Differentially expressed genes were considered significant if the following criteria were met: i) p value <0.05 and ii) absolute fold-change value ≥ 1.2 . The Benjamini Hochberg method³ for false discovery rates was used comparing the computed p values with the adjusted p values and the false discovery rate was calculated to be 0.1. Cluster analysis was performed using average-linkage hierarchical cluster analysis with a correlation matrix. Both expression patterns in individuals and genes were clustered. Gene Ontology (GO) and Kyoto Encyclopedia of Genes and Genomes (KEGG) Pathway analyses were performed using the Genecodis software^{4, 5} <http://genecodis.cnb.csic.es/>. The gene ontology category 'biological process' was selected and the p value calculations were performed using the hypergeometric-distribution statistical test. The p values were then corrected by an implementation of the FDR method of Benjamini and Hochberg as described^{4, 5}.

The DAVID software (<http://david.abcc.ncifcrf.gov/>) was used to analyze GO enrichment of genes involved in transcription regulation and p values were calculated using the Fisher Exact test^{6, 7}. The Venn diagram was performed using Venny (<http://bioinfogp.cnb.csic.es/tools/venny/index.html>). Ingenuity software (Redwood City, CA) was used to analyze enrichment for Biological functions.

Mass spectrometry analyses.

Histone bands were excised from SDS-PAGE gels and digested in-gel as described earlier in ⁸. Briefly, histones were destained and propionylated before trypsin digestion was performed. After digestion, peptides were desalted offline using Carbon carbon TopTips (TT1CAR, Glygen) and reconstituted in 0.1% TFA. Peptides were injected in an Ultimate 3000 HPLC system (LC Packings Dionex) and separated with a gradient from 5% to 60% acetonitrile in 0.1% formic acid over 40min at 300nL/min on a C18 analytical column (75µm ID homepacked with ReproSil-Pur C18-AQ 2.4 µm from Dr. Maisch). The effluent from the HPLC was directly electrosprayed into the LTQ Orbitrap mass spectrometer (Thermo Fisher Scientific). The MS instrument was operated in the data-dependent mode to automatically switch between full scan MS and MS/MS acquisition. Survey full scan MS spectra (m/z 250 – 2000) were acquired in the Orbitrap with resolution R=60 000 at m/z 400. The six most intense peptide ions with charge states between two and five were sequentially isolated (window = 2.0m/z) to a target value of 10000 and fragmented in the linear ion trap by collision-induced dissociation (CID). Fragment ion spectra were recorded in the Orbitrap part of the instrument. For all measurements with the Orbitrap detector, three lock-mass ions from ambient air (m/z = 371.10123, 445.12002, 519.13882) were used for internal calibration. Typical mass spectrometric conditions were: spray voltage 1.4kV; no sheath and auxiliary gas flow; heated capillary temperature 200°C; normalized collision energy 35% for CID in linear ion trap. An activation q=0.25 and activation time of 30ms were used. Peptides were quantified using the peak area from the corresponding extracted ion chromatograms (±10 ppm). Besides H3K9me2/3, no other modifications on H3 showed significant changes when analyzed by MS.

Nissl staining

10 μm frozen sections were air dried at room temperature and then incubated in ethanol-chloroform (1:1) for 20 min, 95% ethanol, 70% ethanol (1-3 min), then rinsed in ddH₂O. Sections were then stained in a 0.5% Cresyl Violet (Sigma). Slides were then rinsed twice in ddH₂O and washed in 70% ethanol, rinsed in 95% ethanol, and then dehydrated in absolute ethanol cleared in xylene and mounted in Permount; sections were analyzed at the microscope (Leica DMI 6000 CS).

Immunohistochemical analyses and cell counts

Immunostaining experiments were performed on 10 μm cryostat coronal brain sections. Slides were firstly incubated in 4% paraformaldehyde in PBS for 20 min; permeabilized in 0.3% Triton in PBS for 10 min, followed by 1 hour pre-incubation with 5% of normal goat serum. Antibodies were incubated overnight in PBS, containing 1% normal goat serum at 4°C. Secondary antibodies were incubated for 2 hours at room temperature (RT). Nuclei were counterstained with Draq5 staining; slides were mounted in Vectashield (Vector laboratories). Draq5 intensity was used as internal control of the experiments in comparing DA-D2RKO and WT sections.

To determine if an altered DA signaling mice might affect the density of neurons in the PFC of DA-D2RKO mice, we analyzed the PFCs of DA-D2RKO and WT mice. Stereological counts were made on regularly spaced (40 μm) 10 μm sections covering the whole rostrocaudal extent (1mm; Bregma 3.5 to 2.5 mm) using the Volocity software 6.3 (Perkin Elmer)⁹. Neurons and interneurons were identified respectively by NeuN and GAD67 immune-positive criteria. Statistical differences were assessed using the Student's t-test.

RNA isolation and qRT-PCR

Primers used for cDNA were the following:

NR4A2 Forward: GGGACGATCCGGGCTCCCTT;
NR4A2 Reverse: CACTACGTGGTGGCTGCCCCG;
Akt1 Forward: ATGAACGACGTAGCCATTGTG;
Akt1 Reverse: TTGTAGCGAATAAAGGTGCCAT;
NR1 Forward: CACTGTGGCTGCTGGTGGGG;
NR1 Reverse: GGGGCACCTTCCCCAATGCC;
FABP7 Forward: TACGGTGGTGGGTAAGACCCG;
FABP7 Reverse: CTAGTGGCAAAGCCCACGCCC;
SFRP1 Forward: ACCCCGCCAATACCACGGA;
SFRP1 Reverse: TGGGCCCCAGCTTCAAGGGT;
KDM4B Forward: AGCGATGGAAACTGAAATGC;
KDM4B Reverse: ACCACATAGGGCCAGTCATC;
KDM4C Forward: GGCTCCTTCAGCAGAGACAC;
KDM4C Reverse: CGCCATTTGACTTGGATGAC;
GAPDH Forward: AGGTCGGTGTGAACGGATTTG;
GAPDH Reverse: TGTAGACCATGTAGTTGAGGTCA.

Chromatin Immunoprecipitation (ChIP)

Following reverse-cross-linking of ChIP experiments, protein:DNA complexes were proteinase K digested and phenol/chloroform extracted and ethanol precipitated. Recovered DNA was subjected to qRT-PCR using the following primers:

NR4A2 promoter Forward: CCATGGCAGGTGGAGCGCATT,
NR4A2 promoter Reverse: AGGCTGCCATCTAAAGGGGCTT.
Akt1 promoter Forward: TTCTCCGGGAGTGGGGTGTGC,
Akt1 promoter Reverse: TCGTCCCAGAAGCCCGACTTG
MyoG promoter Forward: TCTGGCCAAGGACAAGCCGT,
MyoG promoter Reverse: GCCAAGGCAGTGAGAGCCCAA

Acoustic Startle reflex (ASR)

Mice (22-24 mice /genotype) were handled 5 days before the test. Startle reactivity was measured using two startle chambers (SR-Lab, San Diego Instruments, San Diego, CA) with a continuous white background noise of 65 dB; the test was performed as previously described¹⁰. Briefly, after 5 min acclimation to background white noise of 65dB, mice were subjected to 40 trials of ten acoustic stimuli of different decibels (dB) (65, 70, 74, 78, 82, 86, 90, 100, 110 and 120 dB) each lasting 40msec and the startle amplitude was recorded for 65msec (every 1 msec) starting with the onset of the startle stimulus. Each stimulus was presented four times in pseudorandom order within a block of 10 trials. The average inter-trial interval was of 15 sec (ranging from 10 to 20 sec). The maximum startle amplitude recorded during the 65 msec sampling window corrected by the weight of each animal was used as dependent variable for statistical analyses.

Prepulse Inhibition

PPI was measured using the SR-Lab System and performed using standard protocols¹¹. As for ASR, mice (26-29 animals /genotype) were handled for 5 days before the test. Mice were placed into the startle chambers with a 65dB background noise level. All PPI test sessions consisted of startle trials: pulse-alone (40msec, 120dB), pre-pulse trials (pre-pulse + pulse: 20msec pre-pulse/100msec delay/40msec 120dB pulse), and no-stimulus trials (nostim; 65 dB). The acoustic pre-pulse intensities were 3, 6, and 12 dB (68, 71, and 77 dB) above the background noise. Mice were subjected to 5 exposures to the pulse-alone trial at the beginning and the end of each session; acoustic or nostim trials were presented in a pseudorandom order separated by ~ 15 sec. To calculate %PPI we followed exactly the method in¹¹. The maximum startle amplitude was used as dependent variable.

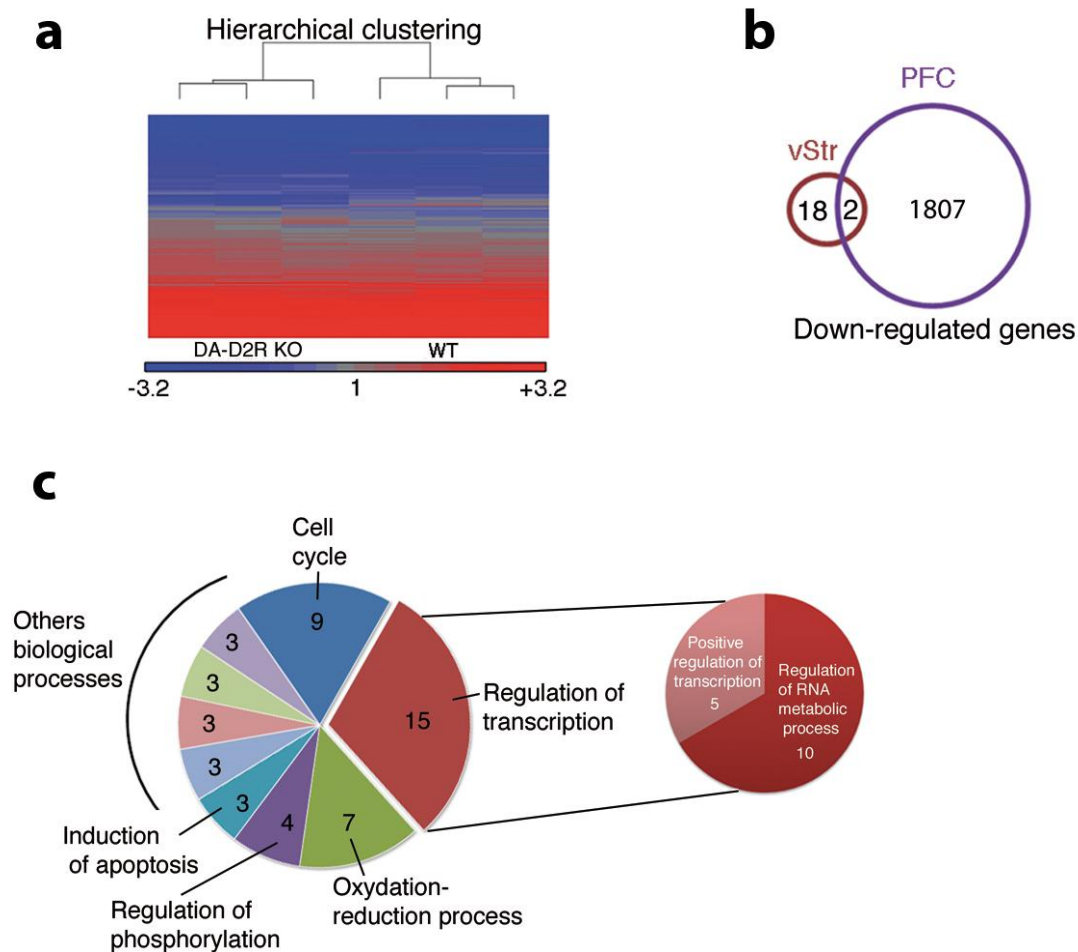
Radial Maze

Before the experiment, mice (14-18 animals/genotype) were food deprived to reach 80-85% of their normal body weight and handled for 1 min for 3 consecutive days. Cocoa Pebbles were used as bait; for acquisition and training we followed the protocol described in ¹². After 6 days of acquisition, the training session started and continued for a total of 15 days, recorded with a video-tracking system (Viewpoint, France). Time to complete the task, working memory errors (reentry into a previously visited arm) and reference memory errors (entry into an arm without bait) were scored and analyzed.

Statistical analyses

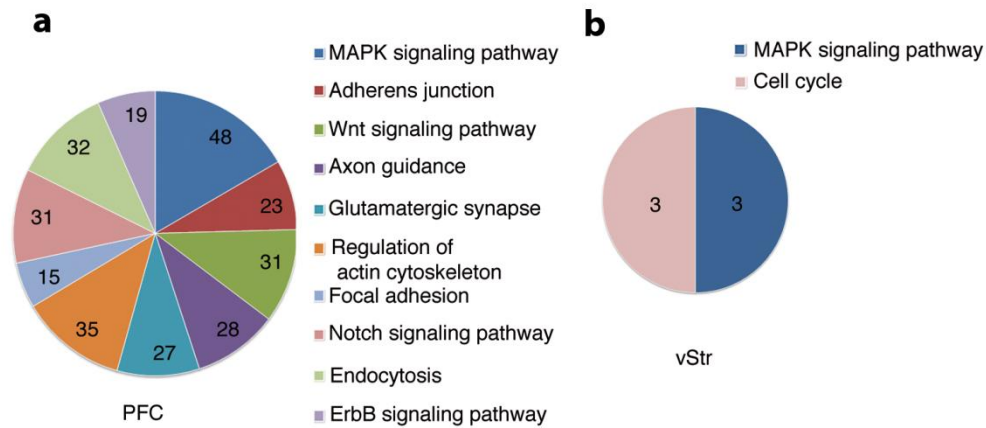
Statistical analyses were performed using: Student's t-test for the analysis of data in Figure 2b, c, f and Figure 3a-e; Two-way ANOVA for Figure 3f and Figure 5a, b, d; and Two-way ANOVA with repeated measures for Figure 4 a-e. For all experiments the appropriate post-hoc analysis was made; $p < 0.05$ was considered statistically significant.

Supplementary Figures:



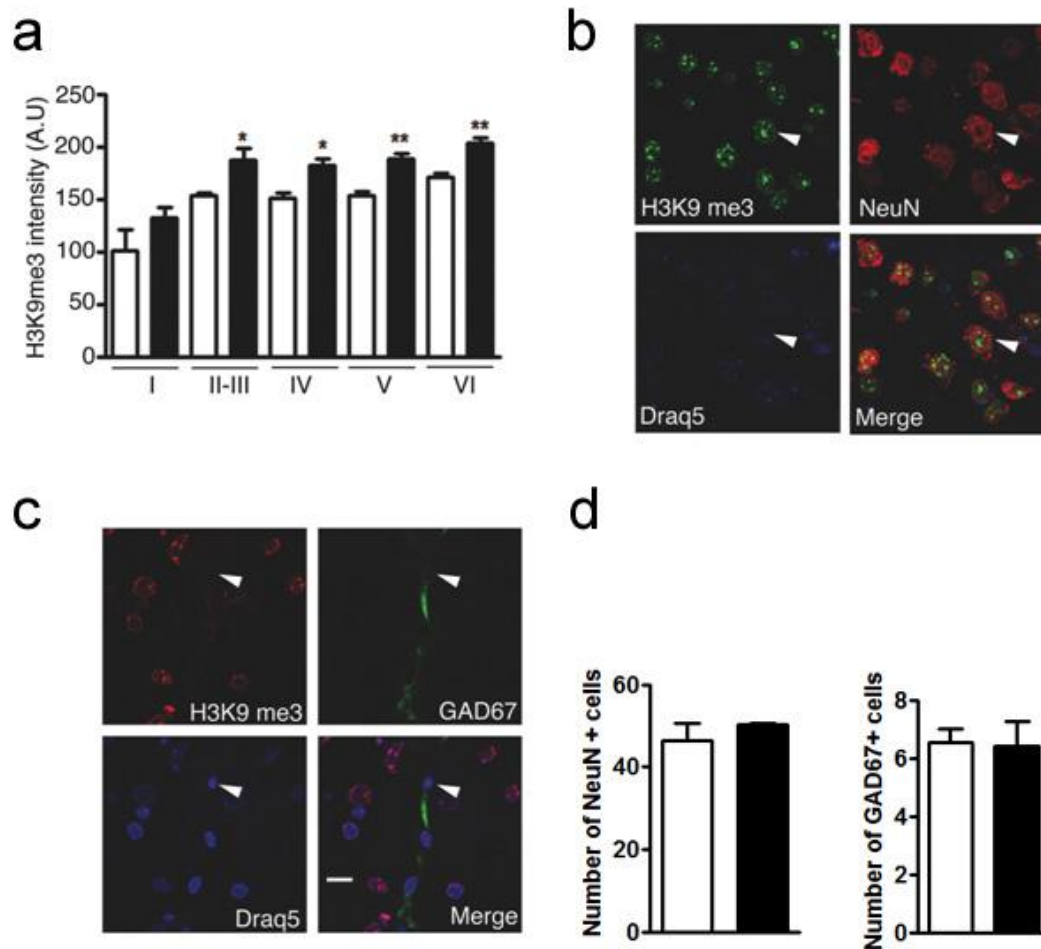
Supplementary Figure 1: Transcriptomic Analyses of the vStr from DA-D2RKO mice.

(a) Heat map representation of genes differentially expressed (fold difference; $p < 0.05$) in the vStr of DA-D2RKO versus WT mice. (b) Venn diagram showing that among the 20 genes down regulated in the vStr only 2 genes overlap with the 1809 annotated genes differentially expressed in the PFC of DA-D2RKO mice. (c) Pie chart (left) of the Biological Processes significantly affected in the vStr transcriptome of DA-D2RKO as compared to WT (Gene Ontology (GO); Genecodis software)(see also Supplementary Table 4). Regulation of transcription contains 15 of the 132 genes, which are either up or down-regulated (Table S2). The pie chart (right) shows that ~67% of these genes are involved in Regulation of RNA metabolic process (10 genes) while ~33% (5 genes) in the positive regulation of transcription.



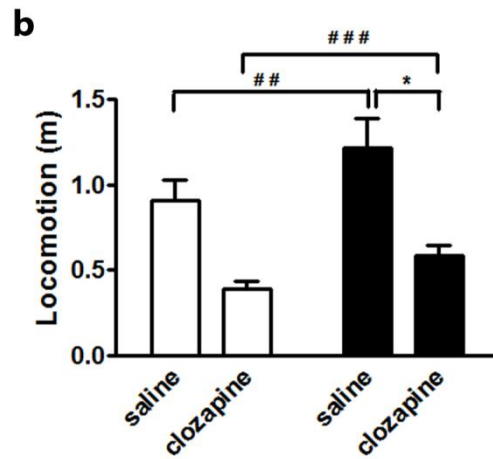
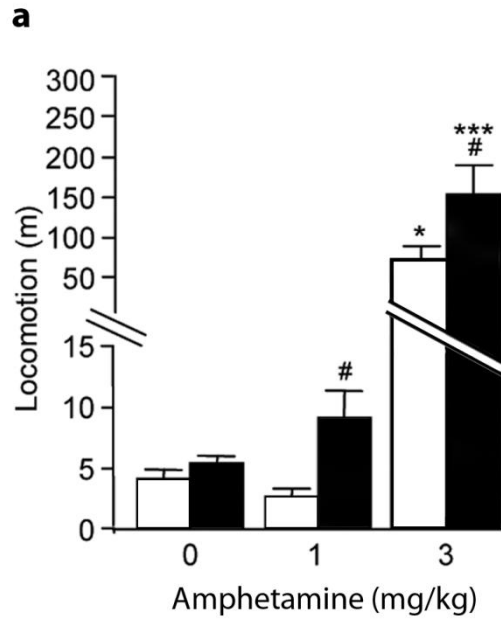
Supplementary Figure 2: KEGG pathways analyses of PFC and vStr of DA-D2RKO mice.

(a) Pie chart representing the 10 most significantly enriched pathways (KEGG) resulting from the analysis of the PFC transcriptome of DA-D2RKO mice (1809 annotated genes; see Supplementary Table 3 for the p values). (b) Pie chart showing the presence of only two enriched pathways (KEGG; $p < 0.05$) in the vStr transcriptome of DA-D2RKO mice (132 annotated genes). These pie charts show that the only enriched pathway in common between PFC and vStr is the MAPK signaling pathway. However, while in the DA-D2RKO PFC 48 genes are differentially expressed in this pathway, only 3 are in the vStr. Moreover, the direction of the differential expression is different between PFC (down-regulation) and vStr (up-regulation) (see Supplementary Tables 1-4).



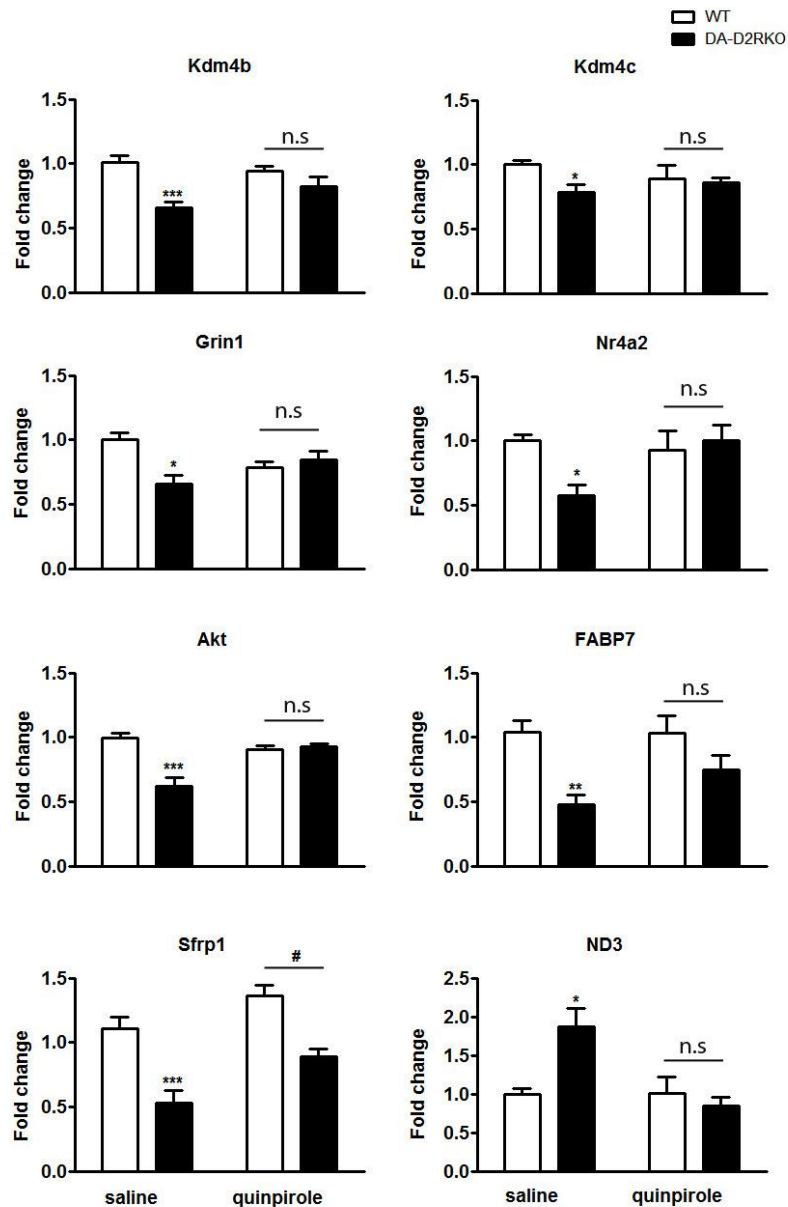
Supplementary Figure 4: Enhanced H3K9me3 in NeuN+ neurons of the DA-D2RKO PFC.

(a) Quantifications of H3K9me3 immunofluorescence intensity per cortical layer of WT (white bars) and DA-D2RKO (black bars) PFCs. Values are expressed as mean of pixels/region of interest (A.U.) from 2 coronal sections (10 μ m)/mouse and a total of 3 mice/genotype. Data are expressed as mean \pm SEM and were analyzed by Student's t-test: WT vs. DA-D2RKO: * p < 0.05, ** p < 0.01. (b) Colocalization of H3K9me3 immunofluorescence (green) and the neuronal marker NeuN (red) in PFC neurons; nuclei are labeled with Draq5 (blue). Scale bar: 10 μ m. (c) Immunofluorescence analyses using H3K9me3 (red) and GAD67 (green) (marker of interneurons) antibodies and Draq5 (blue; marker of nuclei) show that H3K9me3 immunoreactivity in interneurons is below the level of detection. Results shown in S4b and c suggest that the increase of H3K9me3 staining occurs primarily in pyramidal neurons. Scale bar: 20 μ m. (d) Quantification of NeuN⁺ and GAD67⁺ neurons in the PFC of WT (white bars) and DA-D2RKO (black bars) mice. Analyses were performed on serial coronal sections. Data were obtained from the analysis of 25 sections/PFC from 2 mice/genotype and expressed as mean \pm SEM; Student's t-test.



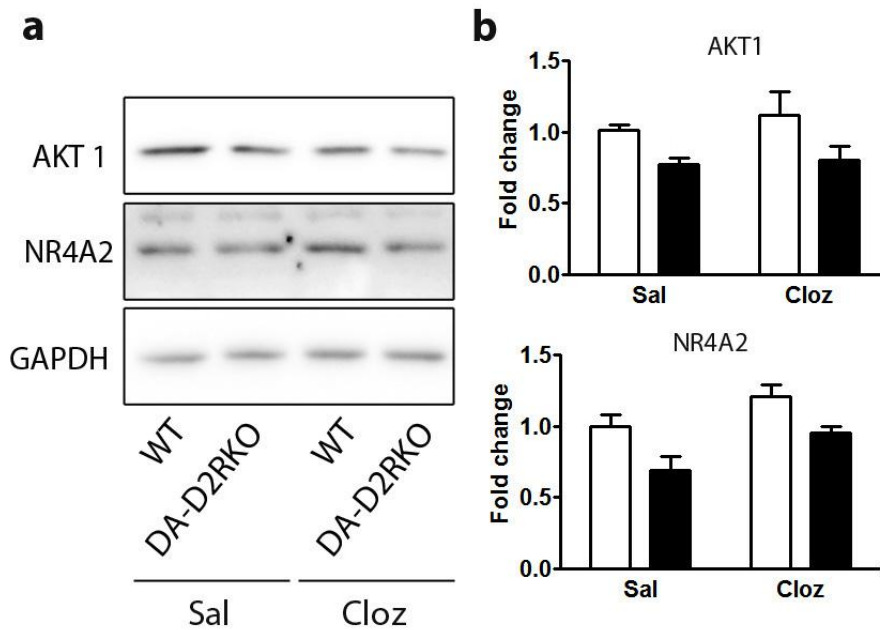
Supplementary Figure 5: DA-D2RKO mice show exaggerated responses to a novel environment and to amphetamine

(a) DA-D2RKO mice are significantly more responsive to the psychomotor effects of amphetamine (1 and 3 mg/kg) than WT mice. Amphetamine (i.p.) was administered in mice habituated for 2 hr to a new home cage; following amphetamine administration activity was recorded for 1 hour. Two-way ANOVA shows a significant [genotype x treatment] interaction ($F_{(2,45)} = 4.606$, $p = 0.016$) ($n = 7-10$). Values are expressed as mean + S.E.M. Bonferroni post-hoc test: Saline vs treated *: $p < 0.05$, ***: $p < 0.001$; WT treated vs DA-D2RKO treated #: $p < 0.05$. (b) DA-D2RKO mice are hyperactive when tested in the open field (OF) as compared to WT¹. The DA-D2RKO hyperactivity is reverted by chronic clozapine treatment. DA-D2RKO and WT littermates were daily injected either with saline or with clozapine (3mg/kg) for 21 days and their motor behavior recorded in the open field (OF) for 15min after the last injection. Two-way ANOVA, Genotype: $F_{(1,27)}=9.11$, $p=0.0055$ and Treatment: $F_{(1,27)}=43.24$, $p<0.0001$; Values are means + SEM; Student's t test: DA-D2RKO saline vs clozapine * $p < 0.05$; WT vs DA-D2RKO ## $p<0.01$; ### $p < 0.001$ ($n = 7-9$).



Supplementary Figure 6: Effect of chronic quinpirole on selected genes mRNA expression in the PFC of DA-D2RKO.

Gene expression analyses in response to quinpirole (15 days, 0.2mg/kg) were performed on genes previously validated by qRT-PCR (Supplementary Table 5). Values are expressed as mean \pm S.E.M. Two-way ANOVA: Kdm4b: $F_{(1,18)}=4.03$, $p=0.0599$. Kdm4c: $F_{(1,18)}=2.66$, $p=0.1376$. Grin1: $F_{(1,18)}=9.21$, $p=0.0084$. Nr4a2: $F_{(1,18)}=5.48$, $p=0.047$. Akt1: $F_{(1,18)}=26.28$, $p=0.0004$. FABP7: $F_{(1,18)}=1.90$, $p=0.2052$. Sfrp1: $F_{(1,18)}=0.30$, $p=0.5915$. ND3: $F_{(1,18)}=6.42$, $p=0.0320$. Bonferroni posthoc analyses showed significant differences between genes from WT and DA-D2RKO saline treated animals, as also reported in Supplementary table 5 (untreated mice). *: $p < 0.05$, **: $p < 0.01$, ***: $p < 0.001$. After chronic quinpirole, Bonferroni post-hoc analyses showed absence of significant differences between genotypes. Sfrp1 was the only gene whose expression was not completely reversed by quinpirole (#: $p < 0.05$).



Supplementary Figure 7: Lack of effect of clozapine on AKT1 and Nr4A2 protein levels in the PFC of DA-D2RKO.

(a) Representative Western-blot analysis of AKT1 and NR4A2 protein levels in the PFC of WT and DA-D2RKO mice chronically treated (21 days) with clozapine (3mg/kg/day). GAPDH was used as control of loading quantities. (b) Quantification of western-blot analyses showing absence of effect of clozapine on AKT1 and NR4A2 protein levels in DA-D2RKO as compared to saline treated mice of the same genotype. Values are means \pm SEM. Statistical analyses showed only a genotype (AKT1: $F_{(1,21)}=13.95$, $p=0.0012$; NR4A2: $F_{(1,21)}=8.17$, $p=0.0126$) but not a genotype x treatment effect (AKT1: $F_{(1,21)}=0.26$, $p=0.6143$; NR4A2: $F_{(1,21)}=0.07$, $p=0.8011$).

SUPPLEMENTARY TABLES

Legend to **Supplementary Table 1:** Genes differentially expressed in the PFC of DA-D2RKO versus WT mice. Significance was set at $p < 0.05$ (Partek software) with a fold change cut off at ± 1.2 .

Legend to **Supplementary Table 2:** Genes differentially expressed in the vStr of DA-D2RKO versus WT mice. Significance was set at $p < 0.05$ (Partek software) with a fold change cut off at ± 1.2 .

Legend to **Supplementary Table 3:** Gene Ontology and KEGG pathway analyses of the DA-D2RKO PFC transcriptome.

Legend to **Supplementary Table 4:** Gene Ontology and KEGG pathway analyses of the DA-D2RKO vStr transcriptome.

Gene symbol	Fold change microarrays	P value microarrays	Fold change qRT-PCR	P value qRT-PCR
KDM4B	-1.24	0.005	-1.32	0.006
KDM4C	-1.21	0.005	-1.18	0.010
Grin1	-1.20	0.014	-1.44	0.020
Nr4a2	-1.51	0.034	-1.59	0.008
Akt1	-1.23	0.023	-1.33	0.049
Fabp7	-1.55	0.029	-1.53	0.024
Sfrp1	-1.54	0.006	-1.71	0.0013
ND3	1.20	0.015	1.94	0.018

Supplementary Table 5: qRT-PCR analyses of mRNA expression of genes differentially expressed in the PFCs of WT and DA-D2RKO mice.

Microarray results were validated on randomly selected genes whose expression was significantly modified in the PFC of DA-D2RKO versus WT mice. Values of qRT-PCR are means \pm SEM, n=5-7/group). Data were analyzed by Student's t test.

ID	FC	p-value	Official gene symbol	pathology	Ref	
Akt1	-1.229	2.40E-02	Thymoma viral proto-oncogene 1; similar ine/threonine protein kinase	Schizophrenia	13	14
Aqp4	-1.21	1.27E-02	aquaporin 4	Schizophrenia	15	16
Atp2b2	-1.213	2.74E-02	ATPase, Ca ⁺⁺ transporting, plasma membrane 2	Schizophrenia	17	
Btg2	-1.309	2.59E-02	B-cell translocation gene 2, anti- proliferative	Schizophrenia	18	
Cadm1	-1.206	2.99E-02	cell adhesion molecule 1	Autism	19	20
Cdkn1b	-1.204	4.57E-02	cyclin-dependent kinase inhibitor 1B	Schizophrenia	21	
Chi3l1	-1.269	1.01E-02	chitinase 3-like 1	Schizophrenia	22	23
Chrm1	-1.244	1.33E-02	cholinergic receptor, muscarinic 1, CNS	Schizophrenia	24	25
Daam2	-1.316	5.12E-02	dishevelled associated activator of morphogenesis 2	Schizophrenia	26	
Dab1	-1.277	3.68E-02	disabled homolog 1 (Drosophila)	Schizophrenia	27	
Dip2c	-1.295	4.47E-02	DIP2 disco-interacting protein 2 homolog C (Drosophila)	ND	28	
Dlg4	-1.242	1.83E-02	discs, large homolog 4 (Drosophila)	Schizophrenia	29	30
Dnmt1	-1.251	1.75E-02	DNA methyltransferase (cytosine-5) 1	Schizophrenia	31	
Egfr	-1.236	7.15E-03	epidermal growth factor receptor	Schizophrenia	32	
ErbB4	-1.254	3.44E-03	v-erb-a erythroblastic leukemia viral oncogene homolog 4 (avian)	Schizophrenia	33	34
Fasn	-1.331	1.98E-02	fatty acid synthase	Schizophrenia	35	
Fgfr1	-1.425	2.02E-03	fibroblast growth factor receptor 1	Schizophrenia	36	
Fxr2	-1.213	1.56E-02	fragile X mental retardation, autosomal homolog 2	FMR	37	
Grik2	-1.204	4.84E-02	glutamate receptor, ionotropic, kainate 2 (beta 2)	Schizophrenia	38	
Grik5	-1.209	2.50E-02	glutamate receptor, ionotropic, kainate 5 (gamma 2)	Schizophrenia	39	
Grin1	-1.208	1.42E-02	glutamate receptor, ionotropic, NMDA1 (zeta 1)	Schizophrenia	40	
Grin2b	-1.212	3.30E-02	glutamate receptor, ionotropic, NMDA2B (epsilon 2)	Schizophrenia	41	42
Grin2c	-1.21	4.40E-03	glutamate receptor, ionotropic, NMDA2C (epsilon 3)	Schizophrenia	43	
Grin2d	-1.309	3.69E-02	glutamate receptor, ionotropic, NMDA2D	Schizophrenia	44	

			(epsilon 4)		
Hmgcs2	-1.279	2.11E-02	3-hydroxy-3-methylglutaryl-Coenzyme A synthase 2	AD	45
Huwe1	1.218	4.01E-02	HECT, UBA and WWE domain containing 1	Autism	46
Lrp10	-1.264	1.09E-02	low-density lipoprotein receptor-related protein 10	Schizophrenia	47
Lrp4	-1.294	2.74E-03	low density lipoprotein receptor-related protein 4	Schizophrenia	47
Mecp2	-1.269	1.97E-02	methyl CpG binding protein 2	Schizophrenia	48
Ncam1	-1.24	2.27E-02	neural cell adhesion molecule 1	Schizophrenia	49 50
Nr4a2	-1.512	3.49E-02	nuclear receptor subfamily 4, group A, member 2	Schizophrenia	51
Nrg1	-1.201	3.44E-02	neuregulin 1	Schizophrenia	52
Nup62	-1.233	8.87E-03	nucleoporin 62	AD	53
Pdlim5	-1.211	2.98E-02	PDZ and LIM domain 5	Schizophrenia	54
Rcan2	-1.216	2.62E-02	regulator of calcineurin 2	DS	55
Sec24c	-1.259	2.52E-02	Sec24 related gene family, member C (S. cerevisiae)	Schizophrenia	56
sema3f	-1.233	4.29E-02	sema domain, ig domain, short basic domain, secreted, (semaphorin) 3F	FRM	57
Slc12a5	-1.203	2.44E-02	solute carrier family 12, member 5	Schizophrenia	58 59
Slc7a11	-1.327	3.10E-02	solute carrier family 7 cationic amino acid transporter, y+ system, member 11	Schizophrenia	60
Snap23	-1.365	4.78E-02	synaptosomal-associated protein 2	Schizophrenia	61
sox10	-1.238	1.92E-02	SRY-box containing gene 10	Schizophrenia	62
Stat3	-1.244	3.59E-03	similar to Stat3B; signal transducer and activator of transcription 3	Schizophrenia	63
Syde1	-1.283	1.45E-02	synapse defective 1, Rho GTPase, homolog 1 (C. elegans)	AD	64
Syt7	-1.282	1.14E-02	synaptotagmin VII	Parkinson	65
Tcf7l2	-1.26	1.23E-02	transcription factor 7-like 2, T-cell specific, HMG-box	Schizophrenia	66
Thra	-1.257	4.63E-03	thyroid hormone receptor alpha; similar to	AD	67

			thyroid hormone receptor		
Trerf1	-1.307	1.36E-02	transcriptional regulating factor 1	ND	⁶⁸
Vim	-1.258	2.74E-02	Vimentin	Schizophrenia	⁶⁹

Supplementary Table 6: Genes down-regulated in the PFC of DA-D2RKO mice involved in human neurological and psychiatric disorders. Enrichment analysis for Biological functions (Ingenuity software) identifies multiple genes differentially expressed in the PFC of DA-D2RKO as involved in human neuropsychiatric diseases. A majority of the genes have been associated to Schizophrenia in human studies. Abbreviations: ND: Neurological disorder, FRM: Fragile X mental retardation, AD: Alzheimer disease, DS: Down Syndrome.

SUPPLEMENTARY REFERENCES

1. Anzalone A, Lizardi-Ortiz JE, Ramos M, De Mei C, Hopf FW, Iaccarino C *et al.* Dual control of dopamine synthesis and release by presynaptic and postsynaptic dopamine D2 receptors. *J Neurosci* 2012; **32**(26): 9023-9034.
2. Kimmel RA, Turnbull DH, Blanquet V, Wurst W, Loomis CA, Joyner AL. Two lineage boundaries coordinate vertebrate apical ectodermal ridge formation. *Genes Dev* 2000; **14**(11): 1377-1389.
3. Benjamini Y, Hochberg Y. Controlling the False Discovery Rate - a Practical and Powerful Approach to Multiple Testing. *J Roy Stat Soc B Met* 1995; **57**(1): 289-300.
4. Nogales-Cadenas R, Carmona-Saez P, Vazquez M, Vicente C, Yang X, Tirado F *et al.* GeneCodis: interpreting gene lists through enrichment analysis and integration of diverse biological information. *Nucleic acids research* 2009; **37**(Web Server issue): W317-322.
5. Carmona-Saez P, Chagoyen M, Tirado F, Carazo JM, Pascual-Montano A. GENECODIS: a web-based tool for finding significant concurrent annotations in gene lists. *Genome Biol* 2007; **8**(1): R3.
6. Huang da W, Sherman BT, Lempicki RA. Bioinformatics enrichment tools: paths toward the comprehensive functional analysis of large gene lists. *Nucleic acids research* 2009; **37**(1): 1-13.
7. Huang da W, Sherman BT, Lempicki RA. Systematic and integrative analysis of large gene lists using DAVID bioinformatics resources. *Nature protocols* 2009; **4**(1): 44-57.
8. Jasencakova Z, Scharf AN, Ask K, Corpet A, Imhof A, Almouzni G *et al.* Replication stress interferes with histone recycling and predeposition marking of new histones. *Molecular cell* 2010; **37**(5): 736-743.
9. Alonso-Vanegas MA, Fawcett JP, Causing CG, Miller FD, Sadikot AF. Characterization of dopaminergic midbrain neurons in a DBH:BDNF transgenic mouse. *The Journal of comparative neurology* 1999; **413**(3): 449-462.
10. Errico F, Rossi S, Napolitano F, Catuogno V, Topo E, Fisone G *et al.* D-aspartate prevents corticostriatal long-term depression and attenuates schizophrenia-like symptoms induced by amphetamine and MK-801. *The Journal of neuroscience : the official journal of the Society for Neuroscience* 2008; **28**(41): 10404-10414.
11. Dulawa SC, Hen R, Scearce-Levie K, Geyer MA. Serotonin1B receptor modulation of startle reactivity, habituation, and prepulse inhibition in wild-type and serotonin1B knockout mice. *Psychopharmacology* 1997; **132**(2): 125-134.
12. Wood MA, Kaplan MP, Brensinger CM, Guo W, Abel T. Ubiquitin C-terminal hydrolase L3 (Uchl3) is involved in working memory. *Hippocampus* 2005; **15**(5): 610-621.
13. Emamian ES, Hall D, Birnbaum MJ, Karayiorgou M, Gogos JA. Convergent evidence for impaired AKT1-GSK3beta signaling in schizophrenia. *Nat Genet* 2004; **36**(2): 131-137.

14. Emamian ES. AKT/GSK3 signaling pathway and schizophrenia. *Front Mol Neurosci* 2012; **5**: 33.
15. Chung TS, Lung FW. Different impacts of aquaporin 4 and MAOA allele variation among olanzapine, risperidone, and paliperidone in schizophrenia. *J Clin Psychopharmacol* 2012; **32**(3): 394-397.
16. Muratake T, Fukui N, Kaneko N, Amagane H, Someya T. Linkage disequilibrium in aquaporin 4 gene and association study with schizophrenia. *Psychiatry Clin Neurosci* 2005; **59**(5): 595-598.
17. Ikeda M, Tomita Y, Mouri A, Koga M, Okochi T, Yoshimura R *et al.* Identification of novel candidate genes for treatment response to risperidone and susceptibility for schizophrenia: integrated analysis among pharmacogenomics, mouse expression, and genetic case-control association approaches. *Biol Psychiatry* 2010; **67**(3): 263-269.
18. Deng X, Takaki H, Wang L, Kuroki T, Nakahara T, Hashimoto K *et al.* Positive association of phencyclidine-responsive genes, PDE4A and PLAT, with schizophrenia. *Am J Med Genet B Neuropsychiatr Genet* 2011; **156B**(7): 850-858.
19. Fujita E, Dai H, Tanabe Y, Zhiling Y, Yamagata T, Miyakawa T *et al.* Autism spectrum disorder is related to endoplasmic reticulum stress induced by mutations in the synaptic cell adhesion molecule, CADM1. *Cell Death Dis* 2010; **1**: e47.
20. Takayanagi Y, Fujita E, Yu Z, Yamagata T, Momoi MY, Momoi T *et al.* Impairment of social and emotional behaviors in Cadm1-knockout mice. *Biochem Biophys Res Commun* 2010; **396**(3): 703-708.
21. Aberg K, Saetre P, Jareborg N, Jazin E. Human QKI, a potential regulator of mRNA expression of human oligodendrocyte-related genes involved in schizophrenia. *Proc Natl Acad Sci U S A* 2006; **103**(19): 7482-7487.
22. Zhao X, Tang R, Gao B, Shi Y, Zhou J, Guo S *et al.* Functional variants in the promoter region of Chitinase 3-like 1 (CHI3L1) and susceptibility to schizophrenia. *Am J Hum Genet* 2007; **80**(1): 12-18.
23. Yang MS, Morris DW, Donohoe G, Kenny E, O'Dushalaine CT, Schwaiger S *et al.* Chitinase-3-like 1 (CHI3L1) gene and schizophrenia: genetic association and a potential functional mechanism. *Biol Psychiatry* 2008; **64**(2): 98-103.
24. Scarr E, Cowie TF, Kanellakis S, Sundram S, Pantelis C, Dean B. Decreased cortical muscarinic receptors define a subgroup of subjects with schizophrenia. *Mol Psychiatry* 2009; **14**(11): 1017-1023.
25. Papaleo F, Lipska BK, Weinberger DR. Mouse models of genetic effects on cognition: relevance to schizophrenia. *Neuropharmacology* 2012; **62**(3): 1204-1220.
26. Kuzman MR, Medved V, Terzic J, Krainc D. Genome-wide expression analysis of peripheral blood identifies candidate biomarkers for schizophrenia. *J Psychiatr Res* 2009; **43**(13): 1073-1077.
27. Verbrugghe P, Bouwer S, Wiltshire S, Carter K, Chandler D, Cooper M *et al.* Impact of the Reelin signaling cascade (ligands-receptors-adaptor complex) on cognition in schizophrenia. *Am J Med Genet B Neuropsychiatr Genet* 2012; **159B**(4): 392-404.

28. DeScipio C, Conlin L, Rosenfeld J, Tepperberg J, Pasion R, Patel A *et al*. Subtelomeric deletion of chromosome 10p15.3: clinical findings and molecular cytogenetic characterization. *Am J Med Genet A* 2012; **158A**(9): 2152-2161.
29. Kristiansen LV, Beneyto M, Haroutunian V, Meador-Woodruff JH. Changes in NMDA receptor subunits and interacting PSD proteins in dorsolateral prefrontal and anterior cingulate cortex indicate abnormal regional expression in schizophrenia. *Mol Psychiatry* 2006; **11**(8): 737-747, 705.
30. Balan S, Yamada K, Hattori E, Iwayama Y, Toyota T, Ohnishi T *et al*. Population-Specific Haplotype Association of the Postsynaptic Density Gene DLG4 with Schizophrenia, in Family-Based Association Studies. *PLoS One* 2013; **8**(7): e70302.
31. Veldic M, Guidotti A, Maloku E, Davis JM, Costa E. In psychosis, cortical interneurons overexpress DNA-methyltransferase 1. *Proc Natl Acad Sci U S A* 2005; **102**(6): 2152-2157.
32. Benzel I, Bansal A, Browning BL, Galwey NW, Maycox PR, McGinnis R *et al*. Interactions among genes in the ErbB-Neuregulin signalling network are associated with increased susceptibility to schizophrenia. *Behav Brain Funct* 2007; **3**: 31.
33. Hahn CG, Wang HY, Cho DS, Talbot K, Gur RE, Berrettini WH *et al*. Altered neuregulin 1-erbB4 signaling contributes to NMDA receptor hypofunction in schizophrenia. *Nat Med* 2006; **12**(7): 824-828.
34. Pan B, Huang XF, Deng C. Antipsychotic treatment and neuregulin 1-ErbB4 signalling in schizophrenia. *Prog Neuropsychopharmacol Biol Psychiatry* 2011; **35**(4): 924-930.
35. Vik-Mo AO, Birkenaes AB, Ferno J, Jonsdottir H, Andreassen OA, Steen VM. Increased expression of lipid biosynthesis genes in peripheral blood cells of olanzapine-treated patients. *Int J Neuropsychopharmacol* 2008; **11**(5): 679-684.
36. Tabares-Seisdedos R, Rubenstein JL. Chromosome 8p as a potential hub for developmental neuropsychiatric disorders: implications for schizophrenia, autism and cancer. *Mol Psychiatry* 2009; **14**(6): 563-589.
37. Bontekoe CJ, McIlwain KL, Nieuwenhuizen IM, Yuva-Paylor LA, Nellis A, Willemsen R *et al*. Knockout mouse model for Fxr2: a model for mental retardation. *Hum Mol Genet* 2002; **11**(5): 487-498.
38. Shibata H, Shibata A, Ninomiya H, Tashiro N, Fukumaki Y. Association study of polymorphisms in the GluR6 kainate receptor gene (GRIK2) with schizophrenia. *Psychiatry Res* 2002; **113**(1-2): 59-67.
39. Shibata H, Aramaki T, Sakai M, Ninomiya H, Tashiro N, Iwata N *et al*. Association study of polymorphisms in the GluR7, KA1 and KA2 kainate receptor genes (GRIK3, GRIK4, GRIK5) with schizophrenia. *Psychiatry Res* 2006; **141**(1): 39-51.
40. Zhao X, Li H, Shi Y, Tang R, Chen W, Liu J *et al*. Significant association between the genetic variations in the 5' end of the N-methyl-D-aspartate receptor subunit gene GRIN1 and schizophrenia. *Biol Psychiatry* 2006; **59**(8): 747-753.

41. Ohtsuki T, Sakurai K, Dou H, Toru M, Yamakawa-Kobayashi K, Arinami T. Mutation analysis of the NMDAR2B (GRIN2B) gene in schizophrenia. *Mol Psychiatry* 2001; **6**(2): 211-216.
42. Li D, He L. Association study between the NMDA receptor 2B subunit gene (GRIN2B) and schizophrenia: a HuGE review and meta-analysis. *Genet Med* 2007; **9**(1): 4-8.
43. Demontis D, Nyegaard M, Buttenschon HN, Hedemand A, Pedersen CB, Grove J *et al*. Association of GRIN1 and GRIN2A-D with schizophrenia and genetic interaction with maternal herpes simplex virus-2 infection affecting disease risk. *Am J Med Genet B Neuropsychiatr Genet* 2011; **156B**(8): 913-922.
44. Choi KH, Zepp ME, Higgs BW, Weickert CS, Webster MJ. Expression profiles of schizophrenia susceptibility genes during human prefrontal cortical development. *J Psychiatry Neurosci* 2009; **34**(6): 450-458.
45. Wollmer MA, Slegers K, Ingelsson M, Zekanowski C, Brouwers N, Maruszak A *et al*. Association study of cholesterol-related genes in Alzheimer's disease. *Neurogenetics* 2007; **8**(3): 179-188.
46. Nava C, Lamari F, Heron D, Mignot C, Rastetter A, Keren B *et al*. Analysis of the chromosome X exome in patients with autism spectrum disorders identified novel candidate genes, including TMLHE. *Transl Psychiatry* 2012; **2**: e179.
47. Gibbons AS, Thomas EA, Scarr E, Dean B. Low Density Lipoprotein Receptor-Related Protein and Apolipoprotein E Expression is Altered in Schizophrenia. *Front Psychiatry* 2010; **1**: 19.
48. Shibayama A, Cook EH, Jr., Feng J, Glanzmann C, Yan J, Craddock N *et al*. MECP2 structural and 3'-UTR variants in schizophrenia, autism and other psychiatric diseases: a possible association with autism. *Am J Med Genet B Neuropsychiatr Genet* 2004; **128B**(1): 50-53.
49. Lyons F, Martin ML, Maguire C, Jackson A, Regan CM, Shelley RK. The expression of an N-CAM serum fragment is positively correlated with severity of negative features in type II schizophrenia. *Biol Psychiatry* 1988; **23**(8): 769-775.
50. Sullivan PF, Keefe RS, Lange LA, Lange EM, Stroup TS, Lieberman J *et al*. NCAM1 and neurocognition in schizophrenia. *Biol Psychiatry* 2007; **61**(7): 902-910.
51. Guillozet-Bongaarts AL, Hyde TM, Dalley RA, Hawrylycz MJ, Henry A, Hof PR *et al*. Altered gene expression in the dorsolateral prefrontal cortex of individuals with schizophrenia. *Mol Psychiatry* 2013.
52. Yang JZ, Si TM, Ruan Y, Ling YS, Han YH, Wang XL *et al*. Association study of neuregulin 1 gene with schizophrenia. *Mol Psychiatry* 2003; **8**(7): 706-709.
53. Sheffield LG, Miskiewicz HB, Tannenbaum LB, Mirra SS. Nuclear pore complex proteins in Alzheimer disease. *J Neuropathol Exp Neurol* 2006; **65**(1): 45-54.
54. Kato T, Iwayama Y, Kakiuchi C, Iwamoto K, Yamada K, Minabe Y *et al*. Gene expression and association analyses of LIM (PDLIM5) in bipolar disorder and schizophrenia. *Mol Psychiatry* 2005; **10**(11): 1045-1055.

55. Branchi I, Bichler Z, Minghetti L, Delabar JM, Malchiodi-Albedi F, Gonzalez MC *et al.* Transgenic mouse in vivo library of human Down syndrome critical region 1: association between DYRK1A overexpression, brain development abnormalities, and cell cycle protein alteration. *J Neuropathol Exp Neurol* 2004; **63**(5): 429-440.
56. Lee SA, Tsao TT, Yang KC, Lin H, Kuo YL, Hsu CH *et al.* Construction and analysis of the protein-protein interaction networks for schizophrenia, bipolar disorder, and major depression. *BMC Bioinformatics* 2011; **12 Suppl 13**: S20.
57. Evans TL, Blice-Baum AC, Mihailescu MR. Analysis of the Fragile X mental retardation protein isoforms 1, 2 and 3 interactions with the G-quadruplex forming semaphorin 3F mRNA. *Mol Biosyst* 2012; **8**(2): 642-649.
58. Hyde TM, Lipska BK, Ali T, Mathew SV, Law AJ, Metitiri OE *et al.* Expression of GABA signaling molecules KCC2, NKCC1, and GAD1 in cortical development and schizophrenia. *The Journal of neuroscience : the official journal of the Society for Neuroscience* 2011; **31**(30): 11088-11095.
59. Tao R, Li C, Newburn EN, Ye T, Lipska BK, Herman MM *et al.* Transcript-specific associations of SLC12A5 (KCC2) in human prefrontal cortex with development, schizophrenia, and affective disorders. *The Journal of neuroscience : the official journal of the Society for Neuroscience* 2012; **32**(15): 5216-5222.
60. Bridges R, Lutgen V, Lobner D, Baker DA. Thinking outside the cleft to understand synaptic activity: contribution of the cystine-glutamate antiporter (System xc-) to normal and pathological glutamatergic signaling. *Pharmacol Rev* 2012; **64**(3): 780-802.
61. Hemby SE, Ginsberg SD, Brunk B, Arnold SE, Trojanowski JQ, Eberwine JH. Gene expression profile for schizophrenia: discrete neuron transcription patterns in the entorhinal cortex. *Arch Gen Psychiatry* 2002; **59**(7): 631-640.
62. Iwamoto K, Bundo M, Kato T. Altered expression of mitochondria-related genes in postmortem brains of patients with bipolar disorder or schizophrenia, as revealed by large-scale DNA microarray analysis. *Hum Mol Genet* 2005; **14**(2): 241-253.
63. Singh RK, Shi J, Zemaitaitis BW, Muma NA. Olanzapine increases RGS7 protein expression via stimulation of the Janus tyrosine kinase-signal transducer and activator of transcription signaling cascade. *J Pharmacol Exp Ther* 2007; **322**(1): 133-140.
64. Zheng Y, Cheng XR, Zhou WX, Zhang YX. Gene expression patterns of hippocampus and cerebral cortex of senescence-accelerated mouse treated with Huang-Lian-Jie-Du decoction. *Neurosci Lett* 2008; **439**(2): 119-124.
65. Glavan G. Intermittent L-DOPA treatment differentially alters synaptotagmin 4 and 7 gene expression in the striatum of hemiparkinsonian rats. *Brain research* 2008; **1236**: 216-224.
66. Hansen T, Ingason A, Djurovic S, Melle I, Fenger M, Gustafsson O *et al.* At-risk variant in TCF7L2 for type II diabetes increases risk of schizophrenia. *Biol Psychiatry* 2011; **70**(1): 59-63.
67. Lauterbach EC. Psychotropic drug effects on gene transcriptomics relevant to Alzheimer disease. *Alzheimer Dis Assoc Disord* 2012; **26**(1): 1-7.

68. Duguay Y, Lapointe A, Lavallee B, Hum DW, Rivest S. Cloning of murine TReP-132, a novel transcription factor expressed in brain regions involved in behavioral and psychiatric disorders. *Mol Psychiatry* 2003; **8**(1): 39-49.
69. Katsel P, Byne W, Roussos P, Tan W, Siever L, Haroutunian V. Astrocyte and glutamate markers in the superficial, deep, and white matter layers of the anterior cingulate gyrus in schizophrenia. *Neuropsychopharmacology* 2011; **36**(6): 1171-1177.